Preparation, X-ray and Spectroscopic Investigations of Europium(III) Trinitrato Complexes with the Macrocycle Derived from 2,6-Diformyl-4-chlorophenol and Diethylenetriamine

J.-C. G. BÜNZLI*, E. MORET

Institut de Chimie Minérale et Analytique, Université de Lausanne, Place du Château 3, Lausanne, Switzerland

U. CASELLATO, P. GUERRIERO and P. A. VIGATO*

Istituto di Chimica e Tecnologia dei Radioelementi C.N.R., Area della Ricerca, Corso Stati Uniti 4, 35100 Padua, Italy

(Received March 14, 1988)

Abstract

The macrocyclic europium(III) complex $[Eu(H_2L)(NO_3)_2]NO_3$, where H_2L is derived from the condensation of 2,6-diformyl-4-chlorophenol and diethylenetriamine, was prepared and crystallized in two forms, yellow and red. The two forms are isostructural but display slightly different spectroscopic properties. The crystal structure of the red form was determined by X-ray crystallography. The compound is monoclinic, space group $C2/c$, with $a = 23.783(3)$, $b = 14.377(3)$, $c = 19.346(3)$ Å, $\beta = 91.76(4)°$; $D_c = 1.69$ g cm^{-3} for $Z = 8$. The structure was refined to $R_f = 0.053$. The europium ion is nine-coordinate, being directly bonded to four oxygen atoms of two bidentate nitrate ions while the third nitrate is ionic. Two oxygen and three nitrogen atoms of the ligand complete the coordination polyhedron. The distances from the metal ion to the bonded atoms are slightly longer than those found for the analogous terbium compound owing to the larger ionic radius of europium. Average distances are: Eu–O(nitrate) 2.50(3) Å, Eu–O(ligand) 2.28(1) Å, Eu–N(ligand) 2.57(3) Å.

Spectroscopic measurements suggest that the difference in colour of the two crystalline forms arises from differences in the stacking of the molecules in the unit cell.

Introduction

The specific spectroscopic and magnetic properties of lanthanide(III) ions have made them essential components in the preparation of new materials [1] and ideal as probes in studies of biological systems [2]. These latter investigations have often been carried out with the help of macrocyclic ligands [3, 4]. For instance, europium(III) has been commonly used as a replacement probe for Ca(II) owing to the analogy between the chemical and physicochemical properties of these two ions [2, 3, 5, 6].

The possibility of using lanthanide(III) ions in the template synthesis of macrocycles, on the basis of the similarity of their ionic radii with those of the alkaline earth metal cations, has been successfully proposed and several papers have been published to test the 4f ions as template devices in condensation reactions [7, 8]. We have recently prepared a series of lanthanide(III) complexes with compartmental Schiff bases derived from 2,6-diformyl-4-chlorophenol and polyamines of the type $NH_2–(CH_2)_2–X–(CH_2)_2–NH_2$ (X = NH, S) with the aim of finding the best conditions and the most appropriate ligand (in terms of type and number of donor atoms, cavity radius, etc.) for the synthesis of homo- and/or heterodinuclear lanthanide complexes [9]. In particular, lanthanide(III) nitrate hydrates and the above formyl and amine precursors gave by template or step-by-step procedures in methanol/chloroform solution, complexes of the type $[Ln(H_2L)(NO_3)_2]NO_3$, where H_2L is the macrocycle shown in Fig. 1.

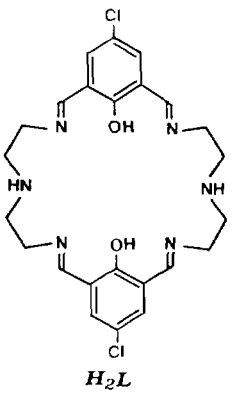

H_2L

Fig. 1. Structure of the macrocycle H_2L.

*Authors to whom correspondence should be addressed.

0020-1693/88/$3.50

Although compartmental, the ligand coordinates only one lanthanide ion in one of the two chambers, while a further cyclization occurs in the free one, as shown by the X-ray structure of the terbium(III) complex [9].

The analogous europium(III) complex has now been isolated as two crystalline forms, a red and a yellow one. Both have the same elemental analyses and are isostructural. In this communication, we present X-ray diffraction and spectroscopic investigations of these two forms of $[Eu(H_2L)(NO_3)_2]NO_3$ with the purpose of revealing the differences between these two complexes and of finding a suitable explanation.

Experimental

2,6-Diformyl-4-chlorophenol was prepared according to ref. 10. 1,5-Diamino-3-azapentane (Aldrich, 95%) was used without further purification. The macrocyclic ligand H_2L was prepared and purified according to literature methods [11, 12].

Preparation of $[Eu(H_2L)(NO_3)_2]NO_3$

Method A

To a methanolic solution (20 ml) of 2,6-diformyl-4-chlorophenol (1 mmol), $Eu(NO_3)_3 \cdot nH_2O$ (0.5 mmol) in methanol (10 ml) and the polyamine $NH_2-(CH_2)_2-NH-(CH_2)_2-NH_2$ (1 mmol) were added dropwise. The volume of the resulting yellow solution was reduced and the yellow–orange precipitate obtained was filtered, washed with diethyl ether and dried *in vacuo*.

Method B

To a suspension of the preformed cyclic Schiff base (1 mmol) obtained according to refs. 11 and 12, in chloroform (20 ml), $Eu(NO_3)_3 \cdot nH_2O$ (1 mmol) in methanol (20 ml) was added. The solution was refluxed for 1 h. The solvent was partially evaporated and the yellow–orange precipitate obtained was treated as above.

By dissolving two portions of the same sample of the complex $[Eu(H_2L)(NO_3)_2]NO_3$, obtained according to method A, in warm dimethylformamide and maintaining the two resulting solutions, after addition of a few drops of methanol, in an atmosphere saturated with diethyl ether, two forms of crystals (yellow and red) were obtained. Both forms were stable in air for a long period of time. They were stored several weeks before X-ray and spectroscopic measurements, and always gave the same elemental analyses (Table I).

X-ray Analyses

Crystals of both the red and yellow forms were mounted on a Philips PW 1100 four-circle diffractometer and reflections were measured at room temperature by the $\theta-2\theta$ scan method (2° min^{-1}), up to $2\theta = 50^\circ$, using graphite-monochromated Mo Kα radiation. The yellow crystal decomposed rapidly preventing any crystal structure determination, contrary to the red crystal (maximum dimension 0.2 mm) which was suitable for X-ray determination. Cell constants of this latter were determined from a least-squares refinement of the setting angles of 25 reflections.

TABLE I. Elemental Analyses for the Yellow and Red Forms of the Complex

Element	Calculated[a] (%)	Found yellow (%)	Found red (%)
C	33.39	33.52	33.50
H	3.17	3.23	3.21
N	15.24	15.23	15.17
Cl	8.57	8.69	8.49
Cl/Eu [b]	2.00	–	–

[a]For $EuC_{23}H_{26}O_{11}N_9Cl_2$. [b]From SEM measurements.

Crystal data are: $[Eu(C_{24}H_{26}O_2N_6Cl_2)(NO_3)_2]NO_3$ (red form), $M = 839.4$ monoclinic, space group $C2/c$, general positions $(0, 0, 0; \frac{1}{2}, \frac{1}{2}, 0); \pm(x, y, z; -x, y, \frac{1}{2} - z)$; $a = 23.783(3)$, $b = 14.377(3)$, $c = 19.346(3)$ Å, $\beta = 91.76(4)^\circ$, $V = 6611$ Å^3, $D_f = 1.67$ g cm^{-1} (by flotation), $D_c = 1.69$ g cm^{-3} for $Z = 8$, μ(Mo Kα) = 21.5 cm^{-1}. A total of 6038 independent reflections were recorded, of which 2130 with $I > 3\sigma(I)$ were considered observed. They were corrected for absorption and Lorenz-polarization [13]. Scattering factors for Eu were taken from ref. 14 and corrections for anomalous dispersion for the other atoms from SHELX [15]; calculations were performed using the SHELX 76 program. The structure was solved by the heavy-atom method and refined by full-matrix least-squares, minimizing the function $\Sigma w(F)^2$ with $w = 1$, to a final R value of 0.053, when the maximum shift of the refined parameters was 0.6σ. The ring carbon atoms were refined as rigid bodies and hydrogen atoms were introduced in calculated positions (C–H = 1.08 Å).

Physicochemical Measurements

FT-IR spectra (150–4000 cm^{-1}) were recorded on a Bruker IFS-113 V interferometer as KBr and polyethylene pellets.

Luminescence spectra and lifetimes were determined at 77 K according to procedures previously described [16].

Chlorine/metal ratios were determined by the integral counting of back-scattered X-ray fluorescence radiation from a Philips Model SEM 505 scanning electron microscope equipped with an EDAX model data station [17]. Samples suitable for SEM analysis

TABLE II. Bond Distances (Å) and Angles (deg) for $[Eu(H_2L)(NO_3)_2]NO_3$ (only coordination)

Distances			
Eu–O(1)	2.48(1)	Eu–O(7)	2.28(1)
Eu–O(2)	2.53(1)	Eu–O(8)	2.28(1)
Eu–O(4)	2.48(2)	Eu–N(3)	2.57(1)
Eu–O(5)	2.48(2)	Eu–N(4)	2.54(2)
		Eu–N(5)	2.58(2)
Angles			
O(1)–Eu–O(2)	51.0(4)	N(3)–Eu–N(4)	68.7(7)
O(4)–Eu–O(5)	50.9(7)	N(4)–Eu–N(5)	64.3(5)
O(7)–Eu–N(3)	72.0(6)	O(7)–Eu–O(8)	96.6(4)
O(8)–Eu–N(5)	73.5(4)		

were prepared by suspending the microcrystalline powders in petroleum ether Some drops of the resulting suspension were placed on a graphite plate and after evaporation of the solvent the samples were metallized with gold or graphite by using an Edward's Model S150 sputter coater [17]. Results are reported in Table I.

Results and Discussion

Structural Investigation

Two crystalline forms (yellow and red) have been recovered by recrystallization of the same sample of $[Eu(C_{24}H_{26}O_2N_6Cl_2)(NO_3)_2]NO_3$, obtained by reaction of $Eu(NO_3)_3 \cdot 6H_2O$ with 2,6-diformyl-4-chlorophenol and diethylenetriamine in a methanol/chloroform solution.

An X-ray investigation of the two forms revealed that they are isostructural. The structure of one form (the red one) was accordingly solved. Bond distances and angles for coordination are given in Table II. The molecular structure is shown in Fig. 2, together with the atom-numbering scheme.

The compound is isomorphous with the terbium analogue previously reported [9] and the differences are ascribed to the larger ionic radius of Eu(III) with respect to Tb(III): 1.120 *versus* 1.095 Å [18] for nine-coordination. As already described for the Tb complex, the central ion is bonded to nine atoms: five donor atoms are from the cyclic ligand and four oxygen atoms from two bidentate nitrate groups; the third nitrate is ionic. These bonds (Eu–O(nitrate), mean 2.50 Å; Eu–O(ligand), mean 2.28 Å; and Eu–N, 2.57 Å) are a little longer than those found in the terbium compound (2.46, 2.25 and 2.54 Å, respectively). The coordination polyhedron may be described as a distorted tricapped trigonal prism, where O(2), O(4) and N(4) are the caps. The edges are slightly longer (mean 0.08 Å) than those found for the terbium complex, with the exception of the bites of the bidentate nitrate groups (O(1)···O(2) and O(4)···O(5)) which are practically unchanged. No relevant differences are found for bond distances

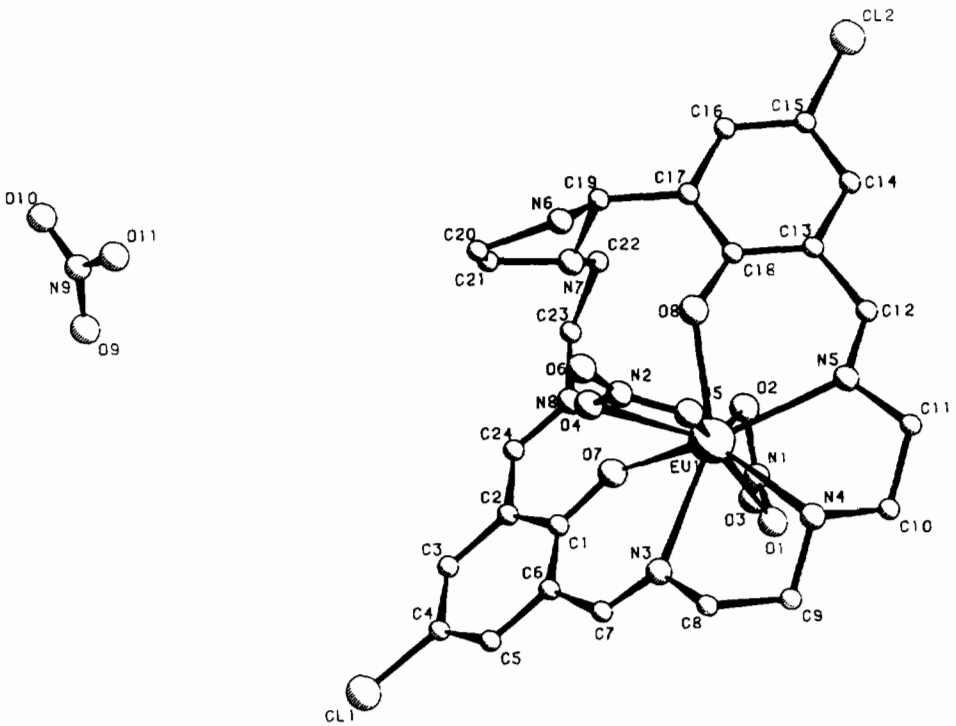

Fig. 2. The molecular structure of $[Eu(H_2L)(NO_3)_2]NO_3$.

and angles in the ligand. Moreover, the pentagon formed by the five coordinated atoms of the ligand presents the same distortion around the europium ion as in the terbium analogue.

Spectroscopic Investigation

Upon grinding, the red complex turns orange. Thereafter, the following three samples were measured:
red (unground) complex, R
orange (red ground) complex, O
yellow (ground) complex, Y

Vibrational Spectra

The IR spectra are identical over the range 4000–400 cm^{-1}. All the bands reported in ref. 9 could be identified. The spectral range 150–350 cm^{-1} exhibits some differences between the two forms Y and O of the complex: (i) the absorption bands around 310–320 cm^{-1} differ in shape; (ii) the orange form has an absorption at 272 cm^{-1} which is shifted to 277 cm^{-1} in the spectrum of the yellow complex; (iii) the broad absorption bands in the Ln–O/Ln–N stretching region are quite different with a maximum at 183 cm^{-1} for the orange form, shifted to 193 cm^{-1} in the spectrum of the yellow complex (these differences could arise from differences in ligand vibrations); (iv) finally, the weak absorptions around 160 cm^{-1} are also slightly different.

Luminescence Spectra

Upon excitation to the $^5L_6$ level (Xe lamp, 395 nm), the spectra of the ground red complex and of the yellow complex are seemingly identical (Fig. 3). The relative intensity of the various transitions is, however, different (*vide infra*). Moreover, the total luminescence intensity of the red sample is less than that of the yellow compound (*ca.* 5 times).

Several excitation spectra of the $^5D_0 \leftarrow {}^7F_0$ transition have been measured with various analysing wavelengths ($^5D_0 \rightarrow {}^7F_1$, $^7F_2$, and $^7F_4$ transitions). Both the O and Y complex forms display very similar spectra. These comprise one main band centered at 17 244 cm^{-1} (width at half height: 7–8 cm^{-1}), and a very weak shoulder around 17 252 cm^{-1}. This would be consistent with one main metal ion site for the Eu(III) ion. The relatively large width of the bands could, however, mean that the ligand displays some fluxionality and that all the molecules have not exactly the same conformation. The shoulder may be interpreted as arising either from a secondary site with a low population or from crystal defects.

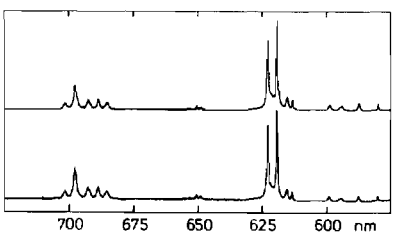

Fig. 3. Luminescence spectra of the yellow (top) and orange (bottom) samples at 77 K. Excitation to the $^5L_6$ level.

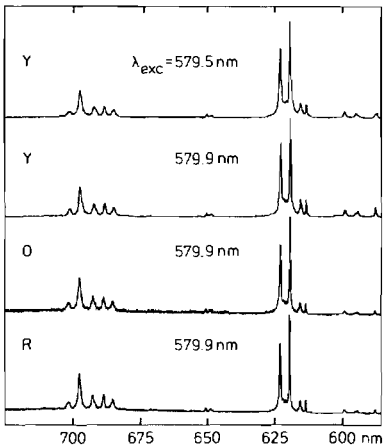

Fig. 4. Laser-excited luminescence spectra of the various forms of the complexes at 77 K (Y = yellow, O = orange, R = red). Excitation: 579.9 nm corresponds to the maximum of the 0–0 transition, 579.5 nm to its shoulder.

The yellow form of the complex has been selectively excited by laser radiation corresponding to both the maximum of the $0 \leftarrow 0$ transition and to its shoulder. The resulting spectra are shown in Fig. 4, along with the spectra of samples R and O, excited at the maximum of their respective $0 \leftarrow 0$ transition.

The overall aspect of the spectra is similar (this is also true for transitions to the $^7F_5$ and $^7F_6$ levels, not shown in Fig. 4). These spectra are typical of species with low symmetry. They are dominated by the electric-dipole, hypersensitive $^5D_0 \rightarrow {}^7F_2$ transition. The relative integrated intensities of the $^5D_0 \rightarrow {}^7F_J$ transitions are listed in Table III.

This suggests a difference between the two complex forms: the intensity of the $0 \rightarrow 2$ and $0 \rightarrow 4$ transitions relative to that of the $0 \rightarrow 1$ transition is much larger for the red form than for the yellow

TABLE III. Relative Integrated Intensities of the $^5D_0 \rightarrow {}^7F_J$ Transitions

J	Yellow complex			Orange complex		Red complex
λ_{exc} (nm)	395	579.9	579.5(sh)	395	579.9	579.9
1	1.0	1.0	1.0	1.0	1.0	1.0
2	10.9	10.3	11.3	17.6	16.0	19.0
3	0.2	0.2	0.2	0.8	0.7	0.7
4	5.3	5.5	5.4	11.3	13.2	15.3
5		0.2	0.2		0.2	
6		0.6	0.6		0.7	

form. In principle, these electric-dipole transitions are forbidden. They gain some intensity because charge-transfer state wavefunctions or vibronic wavefunctions mix with the electronic wavefunctions, making the selection rules obsolete. This mixing is obviously larger for the red form than for the yellow one, a fact confirmed by the reflectance spectra (*vide infra*).

Regarding the two different excitations of the yellow complex, the only difference observed in the resulting luminescence spectra arises in the $0 \rightarrow 1$ transition: excitation on the shoulder produces an extra component on the short wavelength side of the spectrum. Simultaneously, the relative intensity of the two components of the central band is reversed (Fig. 5).

A similar situation is met when the red complex is excited through the shoulder at 579.5 nm. A closer scrutiny of the relative intensities of the three bands of this transition yields the data reported in Table IV.

In principle, three bands are expected for the $0 \rightarrow 1$ transition, having the same intensity as when the metal ion lies on a site with low symmetry. This is the case for both spectra of the yellow complex. However, one band in one spectrum and two bands in the other are seemingly split into two components. Such splittings may arise from interaction between electronic and vibronic levels, leading to a situation similar to that created by Fermi resonances in vibrational spectra [19–21]. For the red complex, one band at 598.8 nm has a slightly larger intensity than the other two. The $^5D_0 \rightarrow {}^7F_2$ transitions of the red and yellow complexes do not exhibit any differences (Fig. 6) and the only observed difference between the two excitations of the yellow complex are small

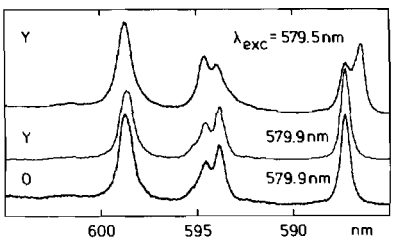

Fig. 5. Luminescence spectra at 77 K: $^5D_0 \rightarrow {}^7F_1$ transition (Y = yellow, O = orange).

TABLE IV. Relative Intensities for the $0 \rightarrow 1$ Transitions

Centre of band (nm)	Yellow		Red (λ_{exc} = 579.9 nm)	
	λ_{exc} = 579.9 (nm)	579.5(sh)	Powder (O)	Crystals (R)
587	0.32	0.33[a]	0.31	0.29
594	0.34[a]	0.33[a]	0.32[a]	0.31[a]
598.8	0.34	0.34	0.37	0.40

[a]Two components.

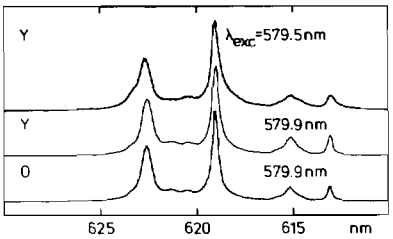

Fig. 6. Luminescence spectra at 77 K: $^5D_0 \rightarrow {}^7F_2$ transition (Y = yellow, O = orange).

changes in the intensities and positions of weak vibronic transitions around 620 nm.

To summarize, both the red and yellow forms of the complex produce the same spectra when excited with the same wavelength, the only difference being the relative intensities of the transitions.

Upon excitation at 579.5 nm (shoulder), both the red and yellow forms still yield similar spectra, but the $^5D_0 \rightarrow {}^7F_1$ transition differs from that obtained when the compounds are excited at the maximum of the $0 \leftarrow 0$ transition (579.9 nm). This is seemingly a second-order effect due to a phenomenon in relationship with laser excitation. In order to shed light on this phenomenon, we have recorded the excitation spectra of the $0 \leftarrow 0$ transition with the analysing wavelength set to the centre of the 'extra' band at 586.5 nm. They are reported in Fig. 7.

As expected, this analysing wavelength creates an increase in the intensity of the shoulders found in Fig. 4. The relative importance of the excitation band at 579.5 nm, with respect to the component at 579.9 nm, is larger for the red crystals than for the orange sample.

The emission spectra of the yellow complex, recorded under seven different excitation conditions spanning the 579.4–579.9 nm spectral range, are displayed in Fig. 8. They show the progressive build-up of the component at 586.5 nm upon shifting the excitation wavelength towards 579.4 nm. It is noteworthy that the relative intensity of the three groups of bands remains unchanged. The extra component,

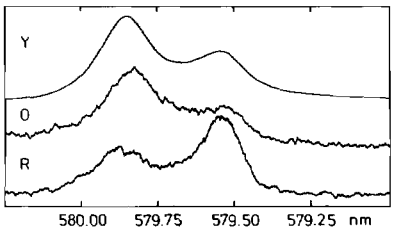

Fig. 7. Excitation spectra of the $^5D_0 \leftarrow {}^7F_0$ transition at 77 K. Analysing wavelength: 586.5 nm, that is, centered on the 'extra' peak of the $^5D_0 \leftarrow {}^7F_1$ transition (Y = yellow, O = orange, R = red).

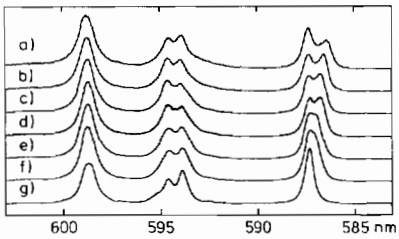

Fig. 8. Luminescence spectra at 77 K: $^5D_0 \rightarrow {}^7F_1$ transition for the yellow sample, recorded under various excitation conditions: (a) 579.36 nm, (b) 579.45 nm, (c) 579.50 nm, (d) 579.55 nm, (e) 579.60 nm, (f) 579.65 nm, (g) 579.86 nm.

e.g. at 586.5 nm, is in fact stealing intensity from the band at 587.3 nm.

A similar situation is met with the red complex. It completely disappears when the excitation wavelength is larger than 579.9 nm. Such behaviour could arise from luminescent traps created by defects in the microcrystals [22].

Lifetimes

Lifetimes of the $^5D_0$ levels were measured by exciting the complexes through the maximum and the shoulders of the $0 \leftarrow 0$ transitions (579.9 nm and 579.5 nm) and with an analysing wavelength of 594 nm ($^5D_0 \rightarrow {}^7F_1$ transition) and 619 nm ($^5D_0 \rightarrow {}^7F_2$ transition). The lifetimes were found to be independent of both the analysing and the excitation wavelengths: yellow complex, 425 ± 7 μs, red complex, 350 ± 6 μs.

The shorter lifetime of the red complex is consistent with its weaker luminescence intensity. This means that quenching processes are more effective in the red than in the yellow complex.

Reflectance Spectra

The reflectance spectra of the three samples studied are markedly different, the red (O, R) samples absorbing more in the 500–650 nm range; one minimum at 430 nm is observed for all three samples, while the minimum at 540 nm is only clearly visible for the red and orange samples.

Conclusions

Red versus Yellow Complex

The IR spectra show some differences between the red and yellow forms either in the conformation of the ligand, or in the arrangement of the coordinating atoms around the Eu(III) ion.

The luminescence study has revealed the following differences between the two forms of the complex: (i) the total luminescence intensity of the red complex is *ca.* 5 times smaller than that of the yellow complex; (ii) the lifetime of the red complex is shorter (350 *vs.* 425 μs); and (iii) the intensities of the $^5D_0 \rightarrow {}^7F_2$ and $^5D_0 \rightarrow {}^7F_4$ transitions, relative to the $^5D_0 \rightarrow {}^7F_1$ transition, are greater in the red complex than in the yellow one.

All these observations are consistent with the presence of a low-lying charge-transfer state in the red complex, which mixes with the $^5D_0$ state, hence the observed quenching and the relative intensities. This is fully confirmed by the reflectance spectrum of the complexes.

Moreover, since the energy of all the transitions from the $^5D_0$ level to the ^7F_J manifold is the same for both the red and the yellow complexes, this means that the Eu(III) ion experiences the same crystal-field effect in both complexes. In other words, its chemical environment is very similar, both in terms of Eu–O and Eu–N distances, and of the coordination geometry.

A possible explanation for the difference in colour could be a different stacking of the molecules in the unit cell allowing, in the case of the red complex, an interaction between the chlorophenol moieties of the ligands. This in turn would influence the energy of the charge-transfer band and, consequently, initiate the quenching phenomena.

This idea is supported by two observations: (i) the slight differences observed in the 150–350 cm^{-1} region of the IR spectra; and (ii) the fact that upon grinding the red complex is transformed into an orange powder, the properties of which are closer to that of the yellow complex.

Vibronic Interactions

This luminescence study has also revealed an interesting although complicated situation with respect to the interaction between the electronic sublevels $^7F_1$ and vibrational levels, leading to additional splittings in the $^5D_0 \rightarrow {}^7F_1$ transition. These depend upon the excitation wavelength and are observed for both the red and yellow forms of the complex. A possible explanation for this lies in the presence of luminescent traps created by small crystal defects.

Supplementary Material

Lists of atomic parameters and the complete lists of bond distances and angles are available from the authors on request.

Acknowledgements

We thank Mr E. Bullita for experimental assistance. We are indebted to Ce.Ri.Ve. Nuova-SAMIM (Venice) for use of facilities for electronic microscopy and X-ray fluorescence microanalysis. J.-C.G.B.

and E.M. thank the Swiss National Science Foundation and the Fondation Herbette (Lausanne) for financial support.

References

1 K. A. Gschneidner, Jr., 'Industrial Applications of Rare Earth Elements', ACS Symposium Series 164, American Chemical Society, Washington D.C., 1981.
2 F. S. Richardson, *Chem. Rev., 82,* 541 (1982).
3 J.-C. G. Bünzli, in K. A. Gschneidner, Jr. and L. Eyring (eds.), 'Handbook on the Physics and Chemistry of Rare Earths', Elsevier, Amsterdam, 1987, pp. 321–394.
4 E. Soini and T. Lövgren, *CRC Crit. Rev. Anal. Chem., 18,* 105 (1987).
5 W. deW Horrocks, Jr. and M. Albin, *Prog. Inorg. Chem., 31,* 1 (1984).
6 J. Buccigross and D. J. Nelson, *J. Less-Common Met., 126,* 343 (1986).
7 P. A. Vigato and D. E. Fenton, *Inorg. Chim. Acta, 139,* 39 (1987).
8 D. E. Fenton and P. A. Vigato, *Chem. Soc. Rev., 17,* 69 (1988).
9 P. Guerriero, U. Casellato, S. Tamburini, P. A. Vigato and R. Graziani, *Inorg. Chim. Acta, 129,* 127 (1987).
10 A. Zinke, F. Hanus and E. Ziegler, *J. Prakt. Chem., 152,* 126 (1939).
11 U. Casellato, D. Fregona, S. Sitran, S. Tamburini, P. A. Vigato and D. E. Fenton, *Inorg. Chim. Acta, 110,* 181 (1985).
12 S. Tamburini, P. A. Vigato and P. Traldi, *Org. Mass Spectrom., 21,* 183 (1986).
13 A. C. T. North, D. C. Phillips and F. S. Mathews, *Acta Crystallogr., Sect. A, 24,* 351 (1968).
14 'International Tables for X-ray Crystallography , Vol. 4, 2nd edn., Kynoch Press, Birmingham, 1974.
15 G. M. Sheldrick, 'SHELX', program for crystal structure determination, University of Cambridge, U.K., 1975.
16 J.-C. Bünzli and G.-O. Pradervand, *J. Chem. Phys., 85,* 2489 (1986).
17 U. Casellato, P. Guerriero, S. Tamburini, P. A. Vigato and R. Graziani, *Inorg. Chim. Acta, 119,* 215 (1986).
18 R. D. Shannon, *Acta Crystallogr., Sect. A, 32,* 751 (1976).
19 J.-C. Bünzli, B. Klein, D. Wessner and N. Alcock, *Inorg. Chim. Acta, 59,* 269 (1982).
20 J.-C. G. Bünzli, G. A. Leonard, D. Plancherel and G. Chapuis, *Helv. Chim. Acta, 69,* 288 (1986).
21 P. Caro, O. K. Moune, F. Antic-Fidancev and M. Lemaître-Blaise, *J. Less-Common Met., 112,* 153 (1985).
22 J.-C. Bünzli, B. Klein, G. Chapuis and K. J. Schenk, *Inorg. Chem., 21,* 808 (1982).